



Isoniazid-Chrysin Incorporated Mixed Ligand Schiff Base Metal(II) Complexes: Synthesis, Spectral Investigation, DNA Binding and Antibacterial Studies

L. RAMGEETHA^{1B} and K. ARUNSUNAI KUMAR^{*1B}

Research Department of Chemistry, VHNSN College (Autonomous), (Affiliated to Madurai Kamaraj University, Madurai), Virudhunagar-626001, India

*Corresponding author: E-mail: arunsunaikumar@vhnsnc.edu.in

Received: 8 October 2023;

Accepted: 16 November 2023;

Published online: 31 December 2023;

AJC-21492

In present work, a novel isoniazid incorporated metal(II) complexes using chrysin as a co-ligand have been synthesized. The structural characterization of all the four transition metal(II) complexes [M = Co²⁺, Ni²⁺, Cu²⁺, Zn²⁺] were investigated by electronic absorption, infrared, ¹H & ¹³C NMR, high resolution electron spray ionization-mass techniques and other physico-chemical parameters. The results revealed that the Schiff base metal complexes with mixed ligands have octahedral configurations. The antibacterial analysis demonstrates that they have exceptional inhibitory efficacy against various bacterial and fungal strains. The DNA study reveals that the Schiff base metal(II) complexes with mixed ligands have intercalation type of binding. The DNA from calf thymus (*ct*-DNA) (PDB ID: 1BNA) was used for molecular docking studies to determine the likely binding location of the metal(II) complexes. The 3D structure of the compounds was optimized using Gaussian 09 software 6-31G/B3LYP set and the DFT calculations were used to locate enzyme-inhibitory areas.

Keywords: Isoniazid, Chrysin, Transition metal(II) complexes, Mixed ligand, DNA binding, Antibacterial activity.

INTRODUCTION

The remarkable stability, chelating, biological and medicinal features of the Schiff base metal complexes have received a lot of interest [1,2]. The coordination compounds especially those belonging to first row transition series such as cobalt(II), nickel(II), copper(II) and zinc(II) complexes exhibit exceptional biological and pharmacological activities [3]. Schiff bases derived from aromatic aldehydes with a hydroxyl group present in *ortho*-position have stimulated the researchers' curiosity due to their capability to serve as bidentate ligands for metal ions. Due to the vast chelating capabilities of Schiff base, it displays a wide range of pharmacological activities [4-6].

Isoniazid also known as isonicotinylhydrazide derivatives are taken into account as a significant class of heterocyclic molecules as they have different activities like antimicrobial, antibacterial and antifungal activities [7]. It is known that compounds with isonicotinoyl groups have been synthesized and analyzed for their chelating and biological features too [8]. Isoniazid is reported to have side effects including increased levels of liver enzymes in blood, liver inflammation and lack of

sensation in hands and feet. Moreover, its side effects can be lessened upon Schiff base formation, which may be attributed due to the deactivation of amino group. Isoniazid is reported with excellent biological applications [7,9]. Chrysin is a phytochemical which belongs to the type of natural polyphenols. The hydroxy group of chrysin binds with different metals, which leads to various applications [10-12].

Mixed ligand coordination complexes could be regarded as a synthetic challenge to tune the characteristics of the transition metal complexes. It is found that the biological activities of the above compounds are enhanced by using mixed ligands [13-15]. Hence, in this work, a Schiff base has been synthesized using salicylaldehyde and isoniazid. Using this Schiff base as the primary ligand and chrysin, the co-ligand, herein four transition metal(II) mixed ligand coordination complexes incorporating the Schiff base containing isoniazid moiety and chrysin are synthesized and characterized using UV, IR, NMR, Molar conductivity, magnetic susceptibility, elemental and mass analyses. The synthesized transition metal(II) complexes are accessed for their DNA binding and antibacterial activities. The results are also compared with the *in silico* methods such

as DFT and molecular docking. The outcomes observed with the mixed Schiff base ligand and its transition metal(II) complexes prove their excellent antimicrobial potency.

EXPERIMENTAL

All the chemicals used were of analytical grade supplied from Sigma-Aldrich, while the metal(II) salts were purchased from E. Merck. All the organic solvents were distilled from appropriate drying agents immediately prior to use.

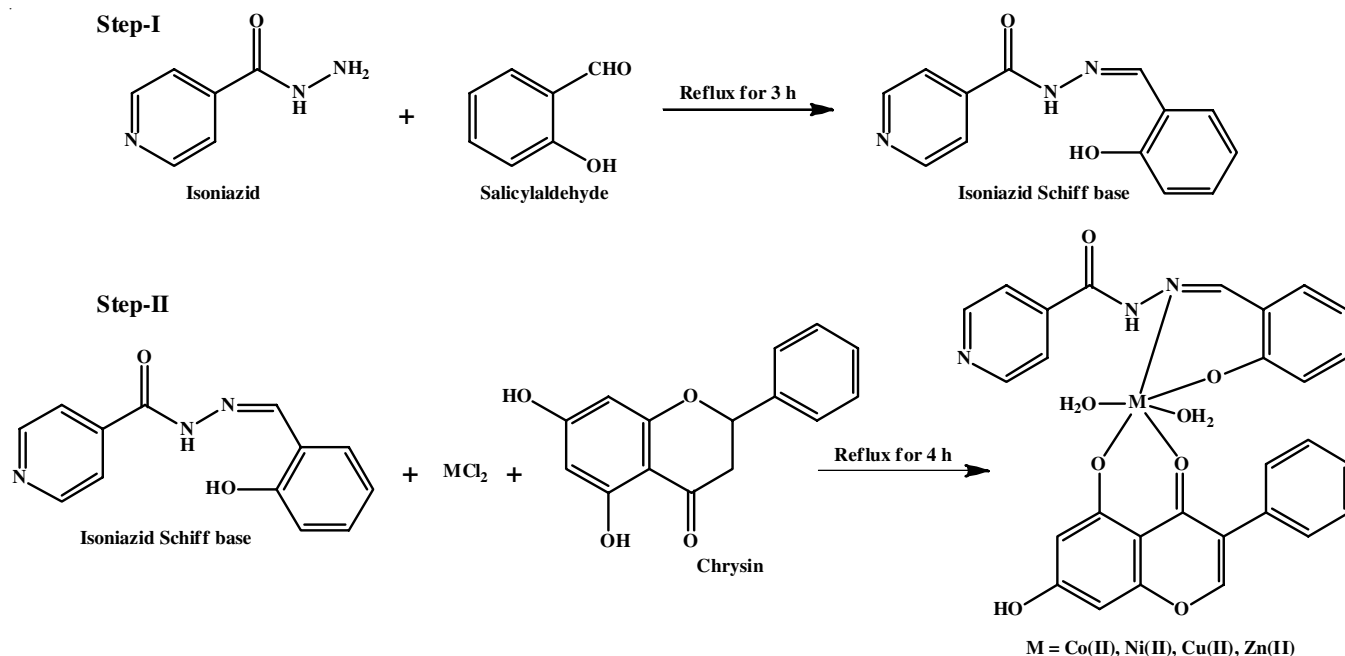
A Perkin-Elmer 240C elemental analyzer was used to perform the elemental analyses on the elements C, H and N. IR analysis was done on Shimadzu FT-IR spectrophotometer using KBr technique in the 4000-400 cm^{-1} range. Using TMS (SiMe_4) as an internal reference, the NMR was captured using a Bruker DPX 300 spectrometer. At room temperature, the JASCO V-530 UV-VIS spectrophotometer was used to detect the absorption spectra. The cyclic voltammetric analysis was done using CHI 620C electrochemical analyzer using acetonitrile as solvent containing 0.2 M TMEDA at 300 K with 10^{-3} M metal complex *via* nitrogen purging. A glassy carbon, a platinum wire and an Ag/AgCl were utilized as the working, counter and reference electrodes. The electrospray ionization was conducted on a MICROMASS Q-TOF mass spectrometer.

Synthesis of Schiff base (L_1): Isoniazid based Schiff base was obtained by treating the 1:1 molar concentration of

isoniazid with salicylaldehyde (10 mmol) dissolved in 30 mL of ethanolic solution. Then the mixture was refluxed for 3 h at 60-80 °C. The colourless precipitate obtained was filtered and dried in vacuum.

Synthesis of mixed ligand Schiff base metal(II) complexes: The isoniazid based Schiff base (L_1) synthesized with the stoichiometry of 1:1 was well-blended with respective metal(II) salt (MCl_2) [$\text{M} = \text{Co(II)/Ni(II)/Cu(II)/Zn(II)}$] in the ethanolic solution for 30 min. Then, 1 mM ethanolic solution of chrysin (L_2) was added into the reaction mixture and continued to stir for 4 h. The reaction mixture was then filtered, dried and recrystallized with hot ethanolic solution (**Scheme-I**). The stoichiometry of the synthesized metal(II) complexes is found to be $[\text{ML}_1\text{L}_2(\text{H}_2\text{O})_2]$ (1:1:1). The physico-chemical data of the mixed ligand Schiff base metal(II) complexes is shown in Table-1.

DNA binding studies: The binding investigation of the prepared metal complexes with deoxyribonucleic acid from calf thymus (*ct*-DNA) were examined in a Tris-HCl buffer (5 mM Tris-HCl/50 mM NaCl) at pH 7.2. The concentration of *ct*-DNA was adjusted from 0 to 10 mM while keeping the volume of synthesized metal(II) complexes (3 mL) constant. The binding constant (K_b), was measured from the Wolf-Shimer equation by plotting the graph between $[\text{DNA}]/(\epsilon_a - \epsilon_f)$ and $[\text{DNA}]$, was determined by allowing the solution to remain at 25 °C for 5



Scheme-I: Synthesis of Schiff base ligand and the mixed ligands metal(II) complexes

TABLE-1
PHYSICO-CHEMICAL PARAMETERS OF THE SYNTHESIZED SCHIFF BASE AND THE METAL(II) COMPLEXES

Compound	Yield (%)	Colour	Elemental analysis (%): Calcd. (found)				m.w.	μ_{eff} (BM)	Λ_m
			M	C	H	N			
$\text{C}_{13}\text{H}_{11}\text{N}_3\text{O}_2$ (L_1)	85	Colourless	–	64.72 (63.93)	4.60 (4.34)	17.42 (17.31)	241.25	–	–
$\text{C}_{28}\text{H}_{23}\text{N}_3\text{O}_8\text{Co}$ (1)	65	Brown	10.02 (9.98)	57.15 (57.13)	3.94 (3.91)	7.14 (7.11)	588.43	5.92	23
$\text{C}_{28}\text{H}_{23}\text{N}_3\text{O}_8\text{Ni}$ (2)	73	Reddish brown	9.98 (9.92)	57.18 (57.14)	3.94 (3.91)	7.14 (7.09)	588.19	2.18	12
$\text{C}_{28}\text{H}_{23}\text{N}_3\text{O}_8\text{Cu}$ (3)	79	Brownish yellow	10.72 (10.68)	56.71 (56.69)	3.91 (3.89)	7.09 (7.02)	593.08	1.86	19
$\text{C}_{28}\text{H}_{23}\text{N}_3\text{O}_8\text{Zn}$ (4)	59	Yellow	10.99 (10.94)	56.53 (56.49)	3.90 (3.88)	7.06 (7.02)	594.88	Diamag.	15

min after adding *ct*-DNA to the mixed ligand metal(II) complex every time.

The Ostwald's micro-viscometer submerged under thermostatically controlled water at a consistent temperature (30 ± 1 °C) was used to measure viscosity. Additionally, fluidity with respect to the time at various concentrations of the synthesized mixed ligand metal(II) complexes, ranging 10-60 mM, were measured while maintaining a DNA concentration of 50 mM. The calculated results were plotted as $(\eta/\eta^0)^{1/3}$ vs. [complex]/[DNA], where η denotes the DNA's inherent viscosity and η^0 denotes DNA's viscosity in the presence of synthetic chemicals [16-18].

DFT studies: The Gaussian 09W software package was employed to optimize geometries of the synthesized compounds in gas phase utilizing B3LYP/6-31+G (d,p) for the ligand and its metal(II) complexes. The input data were visualized and the HOMO-LUMO energies were extracted using the Gaussian view molecular visualization programme. Different chemical reactivity parameters were also estimated using the Koopmans theorem, including chemical potential (μ), global hardness (η), chemical softness (S) and electrophilicity (ω) [19,20].

Antimicrobial assay: All the synthesized mixed ligand metal(II) complexes were examined for their antibacterial efficacy using broth dilution method against Gram-positive bacteria, *S. aureus*, *B. subtilis* and Gram-negative bacteria, *E. coli*, *S. typhi*, *P. vulgaris* and antifungal activity against *A. niger*, *C. albicans*, *C. lunata*, *A. flavus* and *R. bataticola*. The minimum inhibitory concentration values of the synthesized compounds were compared with the standard drugs such as ciprofloxacin and fluconazole [21,22].

RESULTS AND DISCUSSION

The synthesized mixed ligand Schiff base and its metal(II) complexes are stable at room temperature and have higher solubility in common solvents like ethanol, methanol, acetone, etc. whereas, the metal(II) complexes are soluble only in DMSO

and DMF. The absence of any chloride (counter) ion is confirmed *via* Volhard's test.

IR studies: IR band observed in the Schiff base ligand at 1654 cm^{-1} is attributed to the imine ($-\text{CH}=\text{N}$) moiety. The decrease in frequency of the this imine group, observed in all the synthesized metal(II) complexes ($1550\text{-}1525\text{ cm}^{-1}$) indicates the reduction in the double bond character of the C-N bond of the imine moiety. Other additional bands in the ligand and metal(II) complexes at the range $1285\text{-}1270$ and $1580\text{-}1573\text{ cm}^{-1}$ owed to the vibrations of $-\text{C}-\text{O}$ and the carbonyl group present in the isoniazid, respectively (Fig. 1). A wide band observed at 3250 cm^{-1} indicates the water peak in all the complexes. Moreover, the absorption at $560\text{-}525\text{ cm}^{-1}$ range is an indication of M-O bond presence in the metal(II) complexes. Also, the absorption at $492\text{-}484\text{ cm}^{-1}$ is attributed to M-N bond [23,24].

Electronic spectra and magnetic properties: In present study, the electronic spectra of the metal(II) complexes have been analyzed in DMSO solvent and the spectra are reliable with an O_h geometry of the metal(II) complexes. The electronic absorption spectra of the Schiff base ligand and its copper(II) complex are depicted in Fig. 2. For ligand, the band is observed at $40,485\text{ cm}^{-1}$ which is due to the $\pi\text{-}\pi^*$ transition ($-\text{C}=\text{N}$ group). The absorption band detected at $29,411\text{ cm}^{-1}$ is owing to $n\text{-}\pi^*$ transition from the azomethine group [25]. Absorption peak observed at $16,528\text{ cm}^{-1}$ in the copper complex is allotted to $d\text{-}d$ transition (${}^2E_g \rightarrow {}^2T_{2g}$) (Fig. 2), which subsequently confirms the O_h geometry of the copper(II) complex. The experimental magnetic susceptibility value of Cu(II) complex is found to be 1.86 B.M. It is also consistent with the O_h geometry of the complex. In nickel(II) complex, a band is observed at $15,847\text{ cm}^{-1}$, which is due to the ${}^3A_{2g}(F) \rightarrow {}^3T_{1g}(F)$ transition, confirming the O_h geometry of nickel(II) complex. The absorptions at $16,583$ and $17,794\text{ cm}^{-1}$ detected in the electronic spectrum of cobalt(II) complex suggest the ${}^4T_{1g}(F) \rightarrow {}^4T_{2g}(P)$ and ${}^3A_{2g}(F) \rightarrow {}^3T_{2g}(F)$ transitions respectively, which are consistent with the Co(II) octahedral complex. The zinc(II) complex shows

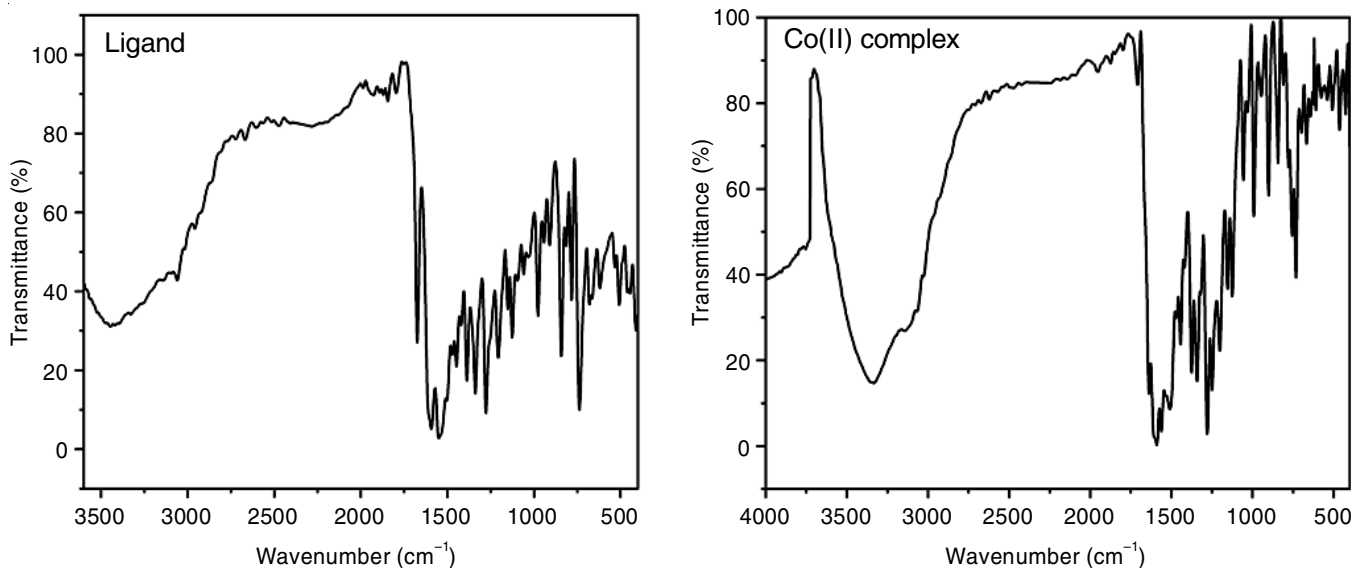


Fig. 1. IR spectra of Schiff base and the cobalt(II) complex

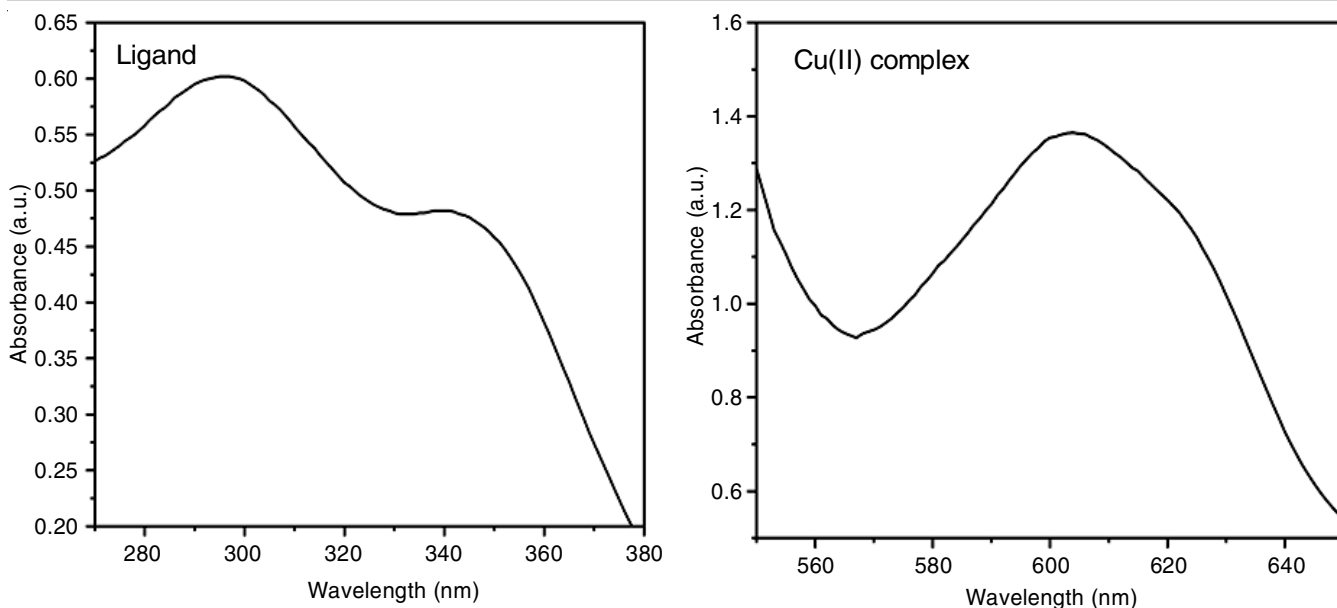


Fig. 2. UV spectra of Schiff base ligand and the copper(II) complex

band at $21,052\text{ cm}^{-1}$ which represents the ligand to metal charge transfer and not $d-d$ transition since it has entirely filled d^{10} configuration. Therefore, the geometry of the zinc(II) complex is confirmed *via* elemental analysis and other characterization methods [26].

Mass spectral studies: The molecular ion peaks and the ESI-mass spectra of the Schiff base and its copper(II) complex are in accordance with the suggested formulae (Fig. 3). The

molecular ion peak for the Schiff base is found at m/z 241, corresponding to $[\text{C}_{13}\text{H}_{11}\text{N}_3\text{O}_2]$ species. Also, the fragments $[\text{C}_{13}\text{H}_{10}\text{N}_3\text{O}]$, $[\text{C}_{13}\text{H}_{13}\text{N}_3]$, $[\text{C}_6\text{H}_7\text{N}_3\text{O}]$ and $[\text{C}_7\text{H}_8\text{N}_2]$ are found at m/z 227, 211, 137 and 120, respectively. The molecular ion peak at m/z 593, observed in the mass spectrum of complex **3**, is consistent with the molecular weight of the complex corresponding to the formula, $\text{C}_{28}\text{H}_{23}\text{CuN}_5\text{O}_8$. The stoichiometry of the complexes is confirmed by the m/z values of the Schiff base

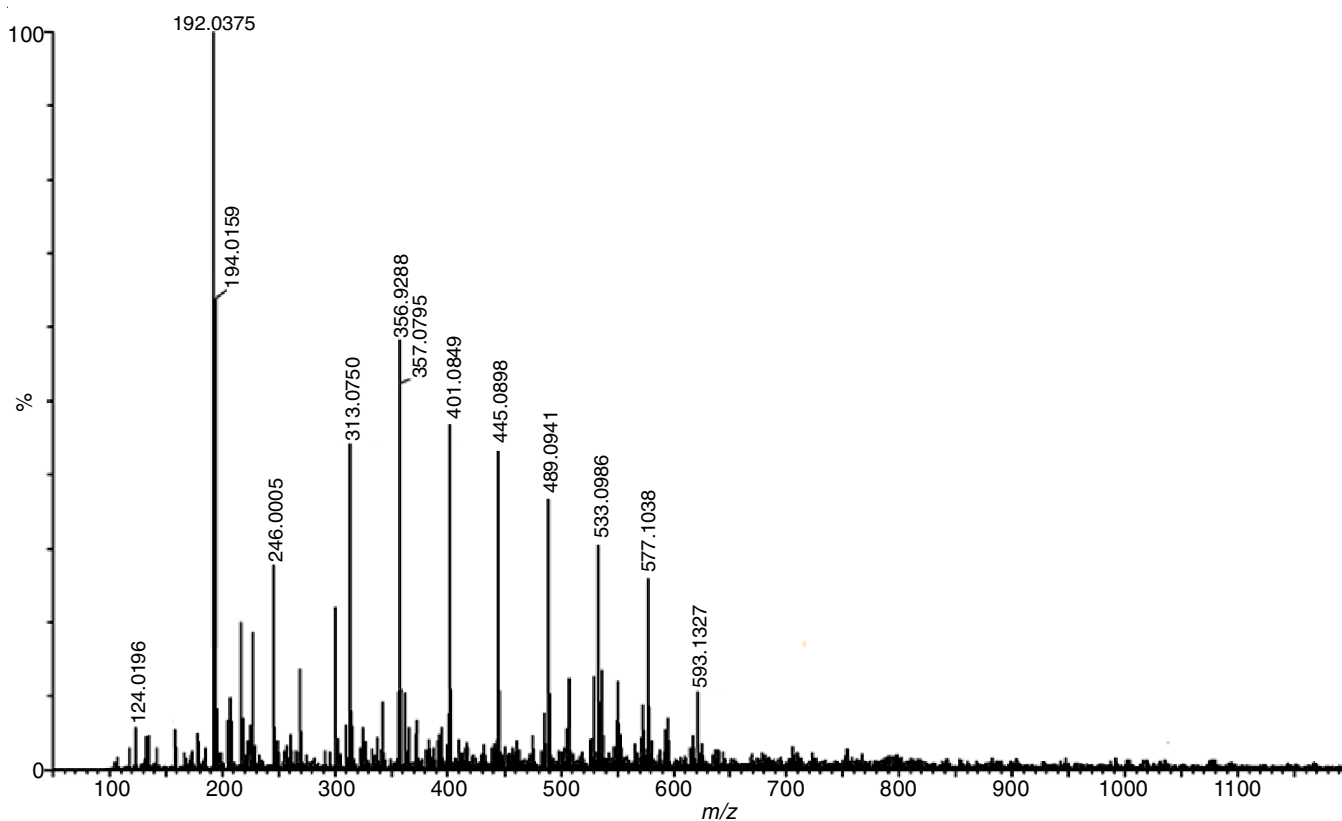


Fig. 3. Mass spectrum of complex **3**

and the components of complex **3**. The detected peaks and their molecular formulae are in good accordance with data obtained from other analytical techniques.

^1H NMR studies: In ^1H NMR study of the ligand and its Zn(II) complex (**4**), the multiplet peaks observed in the range of 7.76 to 7.98 ppm indicate the existence of an aromatic group. The singlet peak at 7.46 ppm is slightly shifted downfield to 7.48 ppm in complex **4**. This shift upon coordination indicates the deshielding mechanism as the azomethine proton binds to the metal ion [27].

^{13}C NMR spectra: In the ^{13}C NMR spectra of Schiff base and its Zn(II) complex (**4**), the peaks detected in the 116-138 ppm range indicates the presence of aromatic carbon. The imine carbon (C=N) peaks are observed at 157 and 159 ppm, in Schiff base and its Zn(II) complex (**4**). These downfield shifts of the peaks were observed upon the chelation of azomethine group (C=N) to the metal ion [28].

Molar conductance: The molar conductance of all the metal(II) complexes was examined using DMSO as solvent at room temperature. The molar conductance values of all of them were observed between 10.5 and 13.4 $\text{ohm}^{-1} \text{cm}^2 \text{mol}^{-1}$. These values support their non-electrolytic nature of the metal(II) complexes [29].

In vitro analysis

DNA binding examination: A decrease in the absorbance of the solution upon enhancing *ct*-DNA concentration denotes the intercalative mode, which encompasses a potent stacking interaction between DNA base pairs and an aromatic chromophore. After adding DNA, the electronic absorption spectra of complexes **1-4** were recorded individually to inspect the influence of the different DNA concentrations (30-150 μM). The percentage of hypochromism was calculated to be in the range of 9.47 to 13.61% and shift in the wavelength was observed to be 1-5 nm, respectively (Table-2) [30]. The observable hypochromism and red shift confirmed the intercalative binding, which is caused by π -stacking of the phenyl rings between the DNA base pairs (Fig. 4). The K_b values of complex **1** > complex **2** > complex **3** > complex **4** were found to be 54.72×10^4 , 5.38×10^4 , 7.36×10^4 , $3.15 \times 10^4 \text{M}^{-1}$, respectively. These findings point toward an intercalative mechanism of interaction between the DNA and the four metal(II) complexes and a higher binding potential of complex **1** [31-33].

Cyclic voltammetric assay: The cyclic voltammetric experiments of the metal(II) complexes in DMSO solvent were conducted in the absence and presence of *ct*-DNA. The positive shift in the electrode potential upon *ct*-DNA additions exhibits

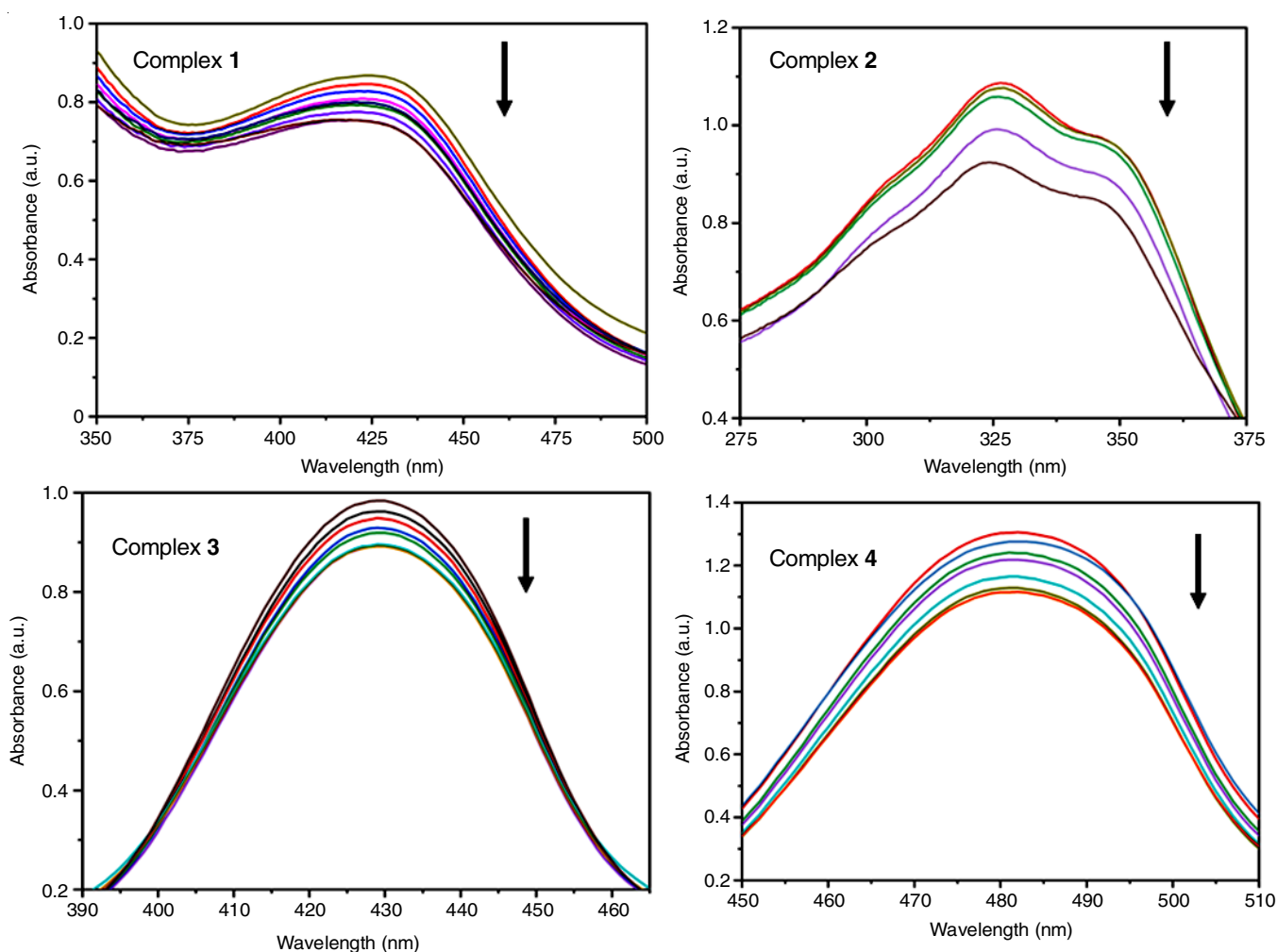


Fig. 4. Absorption changes upon incremental DNA addition. The arrow specifies the direction in which the DNA concentration increases

TABLE-2
ELECTRONIC ABSORPTION SPECTRAL CHARACTERISTICS OF THE COMPLEXES IN THE PRESENCE AND ABSENCE OF *ct*-DNA

Compounds	λ_{\max}		$\Delta\lambda$ (nm)	%H ^a	K_b (M ⁻¹) ^b	ΔG (kJ/mol)
	Free	Bound				
Complex 1	437	433	4	13.61	7.36×10^4	-26.663
Complex 2	322	317	5	12.30	5.38×10^4	-26.988
Complex 3	431	430	1	9.47	4.72×10^4	-27.764
Complex 4	483	481	2	12.9	3.15×10^4	-25.662

^aHypochromism H% = $[A_{\text{free}} - A_{\text{bound}}]/A_{\text{free}} \times 100\%$; ^b K_b = Intrinsic DNA binding constant determined from the UV-vis absorption spectral titration.

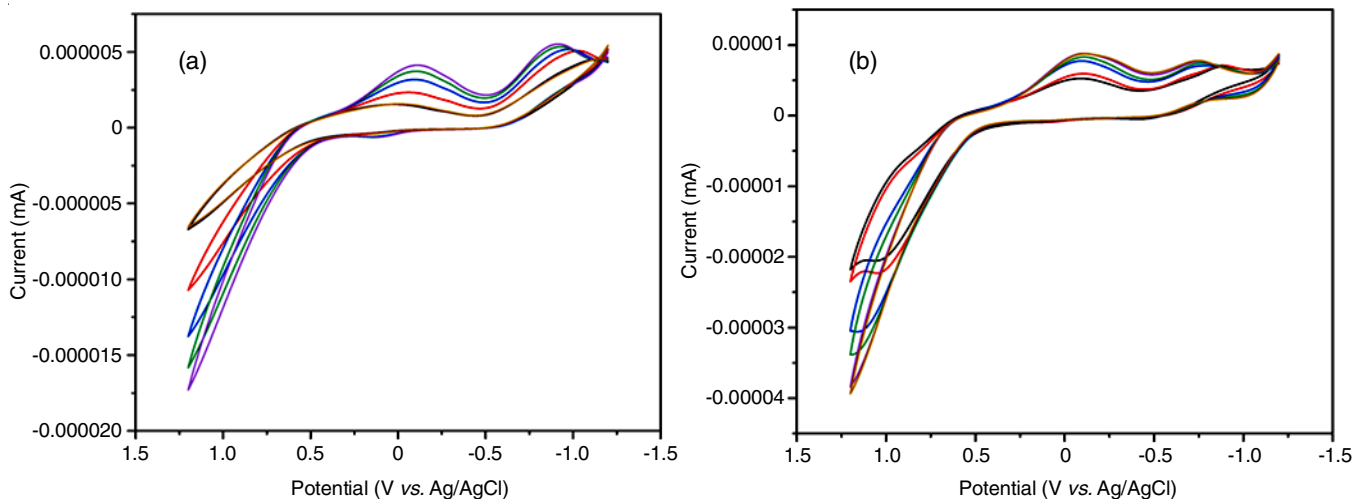


Fig. 5. Cyclic voltammograms of (a) complex 3 and (b) complex 4 in 10^{-3} M DMSO solution buffer (pH = 7.2) at 25 °C in presence of increasing amount of DNA

that the binding mode is intercalation. The cyclic voltammogram of the complexes in the presence and absence of addition of *ct*-DNA is depicted in Fig. 5. During one electron transfer in the redox process of the complexes, the value of I_{pa}/I_{pc} is < 1 , which gives supports that the reaction on the glassy carbon electrode surface is quasi-reversible [34,35]. All the electrochemical parameters are tabulated in Table-3.

TABLE-3
ELECTROCHEMICAL PARAMETERS FOR THE INTERACTION OF DNA WITH THE COMPLEXES

Compound	$E_{1/2}$ (V)		ΔE_p (V)		ip_a/ip_c
	Free	Bound	Free	Bound	
Cobalt(II) complex	0.531	0.546	-0.243	-0.252	0.93
Nickel(II) complex	0.524	0.532	0.223	0.211	0.79
Copper(II) complex	0.621	0.633	-0.487	-0.482	0.88
Zinc(II) complex	0.312	0.334	0.413	0.436	0.92

Viscosity studies: The DNA interaction mechanism of the complexes 1-4 was studied by measuring the viscosity variations upon the increasing concentration of the complexes using ethidium bromide (EB). The increasing viscosity after the addition of the compounds confirms the intercalative binding. The viscosity of DNA plotted against $[\text{complex}]/[\text{DNA}]$ vs. $(\eta/\eta_0)^{1/3}$ is displayed in Fig. 6. The incremental viscosity observed can be attributed to the increase in the length of the DNA helix. The relative viscosity of *ct*-DNA increases in the following order: EB $>$ 3 $>$ 4 $>$ 2 $>$ 1 $>$ ligand (Fig. 6). The results obtained in the viscosity examination is in close agreement with the absorption studies [36,37].

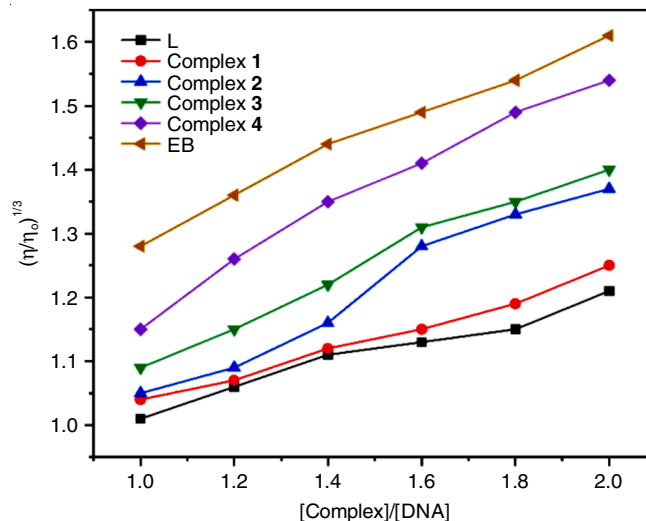


Fig. 6. Consequences of incremental amount of EB and the complexes, on the relative viscosity of *ct*-DNA

Antimicrobial activity: The synthesized Schiff base and its mixed ligand metal(II) complexes were tested for their *in vitro* antibacterial and antifungal activities. The compounds were tested against five fungi viz. *A. niger*, *A. flavus*, *C. lunata*, *R. bataticola* and *C. albicans* as well as Gram-positive bacteria such as *B. subtilis*, *S. aureus* and Gram-negative bacteria such as *S. typhi*, *P. vulgaris* and *E. coli*. Fluconazole and ciprofloxacin were opted as the standard compounds for testing the antifungal and antibacterial activities. From the minimum inhibitory constant values observed, it was observed that the

metal(II) complexes have lower minimum inhibition concentration and hence, higher activity than the ligand (Table-4). This suggestion can be explained *via* Tweedy's chelation and Overtone's concept according to which, they can pass through the lipophilic bacterial membranes and destroy them attributable to the non-polar nature of the metal(II) complexes [38,39].

In silico studies

ADMET properties: Table-5 displays the data from the SWISS-ADME software on the various factors. From the results, it is observed that the compounds obey the Lipinski's rule of five except in terms of molecular weight in case of the synthesized metal(II) complexes. The number of hydrogen bond donors are lesser than 5 and the number of hydrogen bond acceptors are lesser than 10. Furthermore, log P values less than 5, good total polar surface and good solubility values contribute to a good bioavailability score greater than 0.5 attributed to their

polar nature, only the ligand has access to the gastrointestinal tract, whereas metal(II) complexes have minimal gastrointestinal absorption, which may be attributed to the loss of hydroxyl proton during chelation with the metal ions. The synthetic accessibility values of the metal(II) complexes lie in the mid-range of ranking between 0-10 and the value of ligand is 2.26, which denotes that the ligand can be prepared without difficulty [40,41].

DFT studies: The DFT studies were conducted in Gaussian 09W software using B3LYP basis set. The geometry optimization, Frontier molecular orbitals and the reactivity parameters of the synthesized compounds were studied theoretically for the ligand and the mixed ligand metal(II) complexes (**1-4**). Figs. 7 and 8 show the optimized geometry and the Frontier orbitals, *i.e.* HOMO and LUMO images of the synthesized metal(II) complexes, respectively. Table-6 gives the calculated reactivity parameters of the compounds [42].

TABLE-4
ANTIMICROBIAL ACTIVITY OF THE COMPOUNDS

Compound	Minimum inhibitory concentration (μM)									
	Antibacterial activity					Antifungal activity				
	<i>B. subtilis</i>	<i>S. aureus</i>	<i>E. coli</i>	<i>S. typhi</i>	<i>P. vulgaris</i>	<i>A. niger</i>	<i>A. flavus</i>	<i>C. albicans</i>	<i>R. bataticola</i>	<i>C. lunata</i>
Ligand	17.3	18.9	19.2	18.8	25.6	12.5	13.4	15.0	18.6	12.8
Complex 1	15.9	17.8	17.1	16.7	16.6	10.7	12.9	14.5	11.4	11.7
Complex 2	16.2	14.3	18.3	17.8	16.9	11.9	12.2	13.9	11.8	11.5
Complex 3	13.4	14.5	14.4	15.5	15.8	9.4	12.4	13.1	10.1	9.8
Complex 4	16.9	18.1	18.0	15.9	21.1	11.3	13.9	14.5	13.3	12.1
Ciprofloxacin	2.8	1.7	1.9	2.5	2.8	–	–	–	–	–
Fluconazole	–	–	–	–	–	1.3	1.9	2.0	1.3	1.7

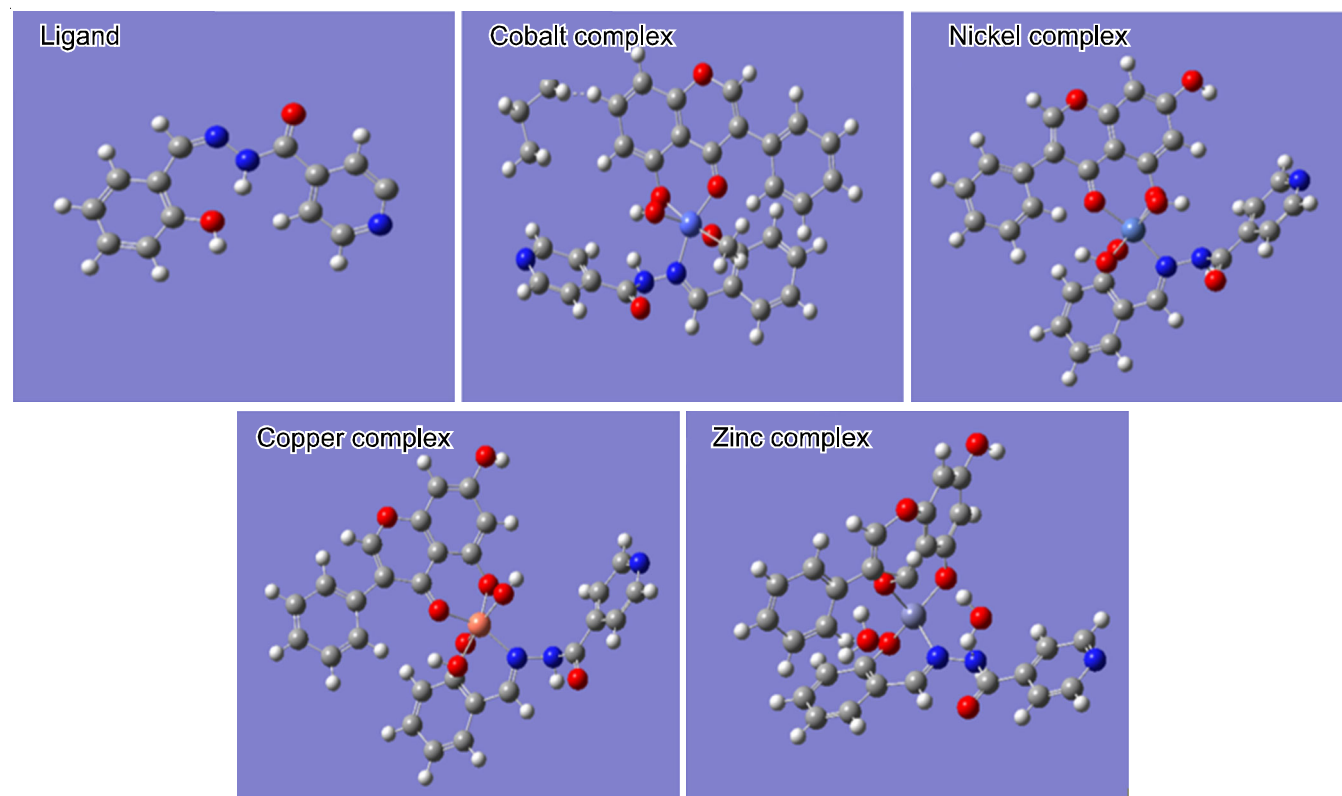


Fig. 7. Optimized structures of Schiff base ligand and the transition metal(II) complexes

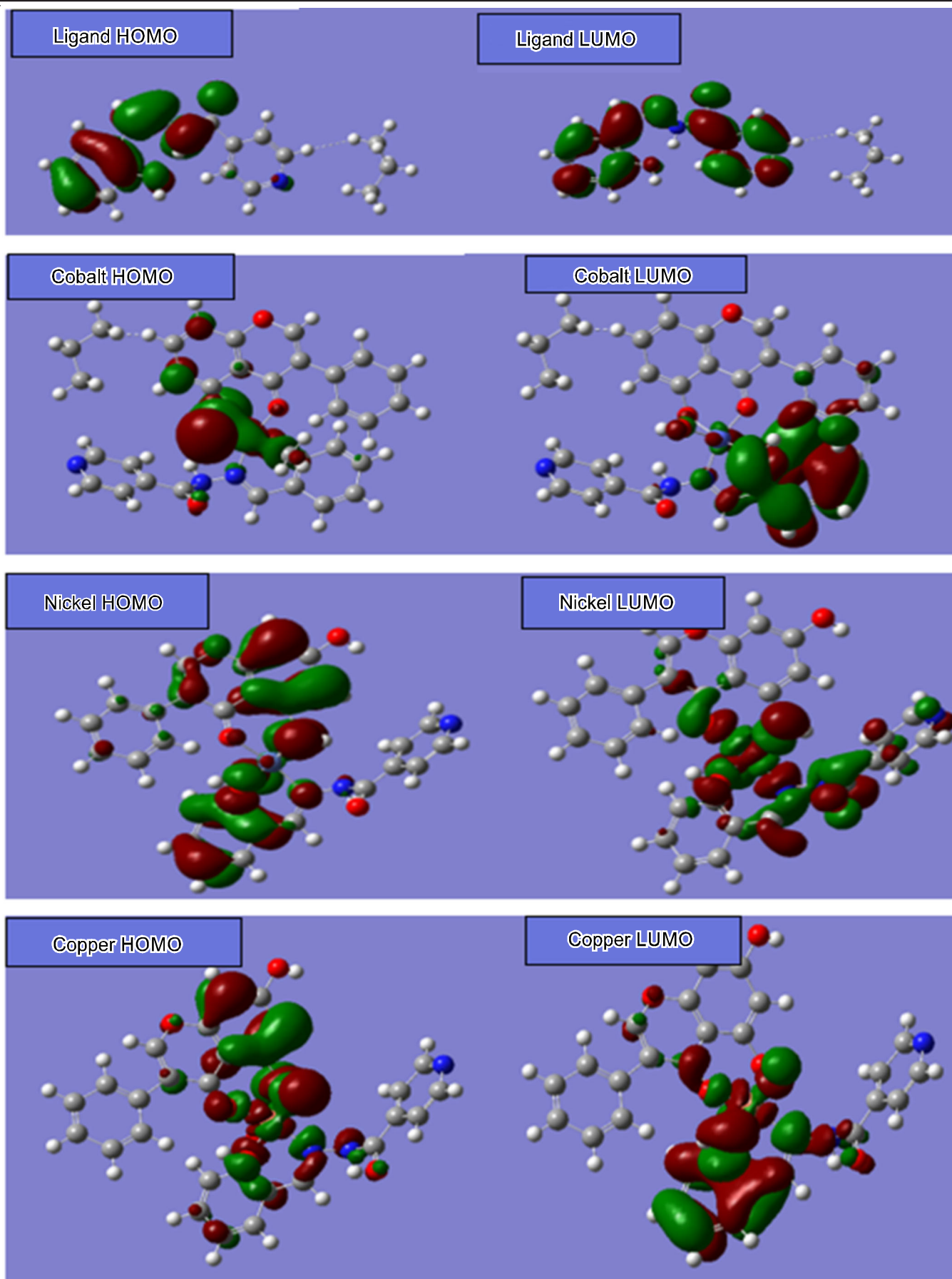


Fig. 8. HOMO-LUMO diagram of the ligand and the metal complexes

TABLE-5
PHYSICO-CHEMICAL PARAMETERS OF THE COMPOUNDS OBTAINED FROM THE SWISS-ADME

Parameters	Ligand	Cobalt complex	Nickel complex	Copper complex	Zinc complex
Molecular weight (g/mol)	241.25	568.44	586.18	591.03	592.03
Number of hydrogen bond acceptor	4	9	9	9	9
Number of hydrogen bond donor	2	4	4	4	4
Number of rotatable bonds	4	4	4	4	4
Topological polar surface area (Å) ²	74.58	119.34	159.80	159.80	159.80
MLog P	0.79	1.17	0.52	0.56	0.52
Gastrointestinal absorption	High	Low	Low	Low	Low
Bioavailability score	0.55	0.56	0.11	0.11	0.11
Synthetic accessibility	2.26	5.32	5.05	5.31	5.68

In HOMO, the electron density is localized over the azo-methine group and the other heteroatoms of the ligand and all the metal(II) complexes (**1-4**) whereas the LUMO is localized at the regions around the coordination sites of Co(II), Cu(II), Ni(II) and Zn(II) complexes. The negative HOMO and LUMO values indicate the stability of the compounds. The higher ΔE (eV) values of the metal(II) complexes (**1-4**) than that of ligand indicate the fact that the complexes are more stable, harder than the ligand. The soft nature of the ligand denotes its stability and higher reactivity towards the coordination site of the metal(II) complexes. The ligand has the greatest dipole moment values among all the compounds indicating its efficiency to cross the biological membranes and its strongest biological interaction [43].

Molecular docking studies: The molecular docking investigation was conducted using the 1BNA receptor retrieved from the <https://www.rcsb.org> site. The docking studies were investigated in Hex 8.0 software and visualized in the Discovery Studio Visualizer 4.0. Both the Schiff base ligand and the mixed ligand metal(II) complexes (**1-4**) interacted with the receptor through hydrogen bonding. The compounds support the intercalative binding mode of the all the compounds, since the compounds stack between the base pairs of DNA. The binding energies of docked compounds were observed as -233.54 (L₁), -344.32 (complex **1**), -308.86 (complex **2**), -332.31 (complex **3**) and -268.72 (complex **4**) kJ mol⁻¹ respectively. The 2D and the 3D interactions of the compounds with the 1BNA receptor are shown in Fig. 9. From the binding constant values, the cobalt(II) complex is found to have profound interactions with the DNA, which also well agreed with the *in vitro* absorption spectroscopic studies [44,45].

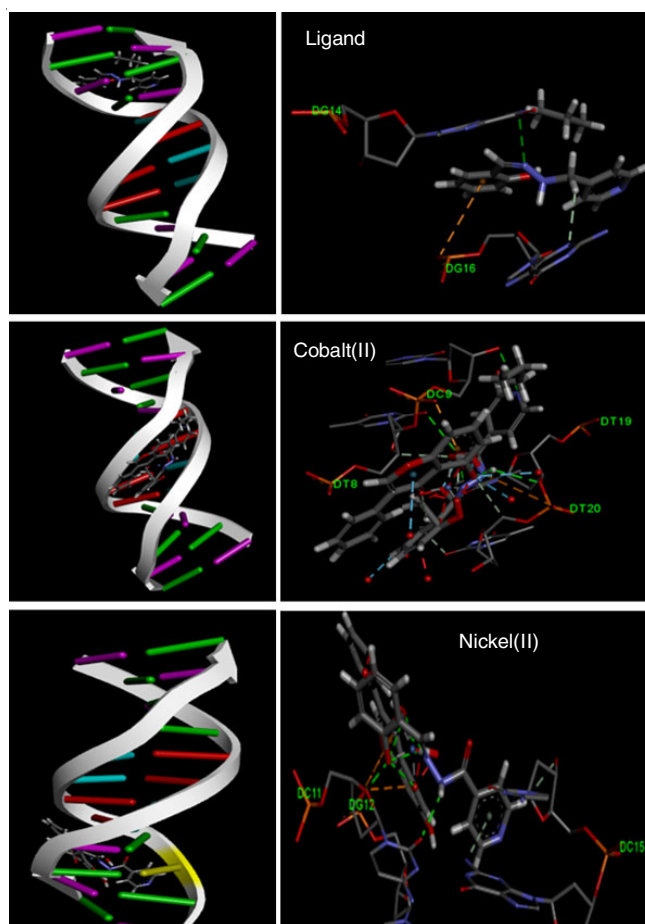


Fig. 9. 2D and 3D interactions of the compounds with the DNA (PDB ID: 1BNA) receptor

TABLE-6
MOLECULAR MECHANICS DATA OF SCHIFF BASE AND COMPLEXES (**1-4**) IN GAUSSIAN SOFTWARE-09W

Parameter	Schiff base	[CoL ₁ L ₂ (H ₂ O) ₂]	[NiL ₁ L ₂ (H ₂ O) ₂]	[CuL ₁ L ₂ (H ₂ O) ₂]	[ZnL ₁ L ₂ (H ₂ O) ₂]
Dipole moment (Debye)	8.09	7.39	4.13	6.34	8.13
HOMO	-6.28	-4.78	-5.65	-5.59	-5.83
LUMO	-1.96	-2.32	-3.17	-3.27	-3.39
ΔE (eV)	4.32	2.45	2.48	2.32	2.44
Electronegativity (χ)	4.12	3.55	4.41	4.43	4.61
Global hardness (η)	2.16	1.23	1.24	1.16	1.22
Electrophilicity (ω)	1.08	0.92	0.62	0.58	0.61
Chemical potential (μ)	-2.16	-1.23	-1.24	-1.16	-1.22
Global softness (π)	0.46	0.81	0.80	0.86	0.82

Conclusion

The present work mainly focuses the synthesis of mixed ligand of transition metal(II) complexes obtained from the condensation of isoniazid and salicylaldehyde (as primary ligand) and chrysin as co-ligand. The synthesized metal(II) complexes were characterized by using different analytical and spectroscopic methods. All the mixed ligand of metal(II) complexes have octahedral geometry. The optimized geometry and the theoretical reactivity parameters were obtained with the help of Gaussian 09 W software. The biological and other pharmacokinetic properties of the compounds were retrieved from the SWISS-ADME software. These complexes were examined for their *in vitro* antimicrobial activity and *ct*-DNA interaction. The intercalating ability of the synthesized compounds was investigated by electronic absorption titrations and viscosity measurements and confirmed by the molecular docking investigations.

ACKNOWLEDGEMENTS

The authors express their sincere gratitude to the VHNSN College Managing Board, The Principal and Head, Department of Chemistry for providing the research facilities and their moral support.

CONFLICT OF INTEREST

The authors declare that there is no conflict of interests regarding the publication of this article.

REFERENCES

- C. Boulechfar, H. Ferkous, A. Delimi, A. Djedouani, A. Kahlouche, A. Boublia, A.S. Darwish, T. Lemaoui, R. Verma and Y. Benguerba, *Inorg. Chem. Commun.*, **150**, 110451 (2023); <https://doi.org/10.1016/j.inoche.2023.110451>
- J. Ceramella, D. Iacopetta, A. Catalano, F. Cirillo, R. Lappano and M.S. Sinicropi, *Antibiotics*, **11**, 191 (2022); <https://doi.org/10.3390/antibiotics11020191>
- D.C. Crans and K. Kostenkova, *Commun. Chem.*, **3**, 104 (2020); <https://doi.org/10.1038/s42004-020-00341-w>
- A.K. Jangid, R. Solanki, S. Patel, K. Medicherla, D. Pooja and H. Kulhari, *ACS Omega*, **7**, 15919 (2022); <https://doi.org/10.1021/acsomega.2c01041>
- A.A. Mohamed, F. Ahmed, W.A. Zordok, W.H. El-Shwiniy, S.A. Sadeek and H.S. Elshafie, *Inorganics*, **10**, 177 (2022); <https://doi.org/10.3390/inorganics10110177>
- N. Kerru, L. Gummidi, S. Maddila, K.K. Gangu and S.B. Jonnalagadda, *Molecules*, **25**, 1909 (2020); <https://doi.org/10.3390/molecules25081909>
- V. Judge, B. Narasimhan and M. Ahuja, *Med. Chem. Res.*, **21**, 3940 (2012); <https://doi.org/10.1007/s00044-011-9948-y>
- F. Rizvi, M. Khan, A. Jabeen, H. Siddiqui and M.I. Choudhary, *Sci. Rep.*, **9**, 6738 (2019); <https://doi.org/10.1038/s41598-019-43082-0>
- F.A.R. Rodrigues, I.S. Bomfim, B.C. Cavalcanti, C.Ó. Pessoa, J.L. Wardell, S.M.S.V. Wardell, A.C. Pinheiro, C.R. Kaiser, T.C.M. Nogueira, J.N. Low, L.R. Gomes and M.V.N. de Souza, *Bioorg. Med. Chem. Lett.*, **24**, 934 (2014); <https://doi.org/10.1016/j.bmcl.2013.12.074>
- M. Kabak, A. Elmali and Y. Elerman, *J. Mol. Struct.*, **477**, 151 (1999); [https://doi.org/10.1016/S0022-2860\(98\)00604-8](https://doi.org/10.1016/S0022-2860(98)00604-8)
- A.C. González-Baró, R. Pis-Diez, B.S. Parajón-Costa and N.A. Rey, *J. Mol. Struct.*, **1007**, 95 (2012); <https://doi.org/10.1016/j.molstruc.2011.10.026>
- V. Ferraresi-Curotto, G.A. Echeverría, O.E. Piro, R. Pis-Diez and A.C. González-Baró, *Spectrochim. Acta A Mol. Biomol. Spectrosc.*, **137**, 692 (2015); <https://doi.org/10.1016/j.saa.2014.08.095>
- T. Khan, S. Raza and A.J. Lawrence, *Russ. J. Coord. Chem.*, **48**, 877 (2022); <https://doi.org/10.1134/S1070328422600280>
- D. Kumar, V.K. Singh and A. Srivastava, *Asian J. Biochem. Pharm. Res.*, **4**, 193 (2014).
- O.A. Dar, S.A. Lone, M.A. Malik, F.M. Aqlan, M.Y. Wani, A.A. Hashmi and A. Ahmad, *Heliyon*, **5**, e02055 (2019); <https://doi.org/10.1016/j.heliyon.2019.e02055>
- M. Kushiro, H. Hatabayashi, Y. Zheng and K. Yabe, *Mycoscience*, **58**, 85 (2017c); <https://doi.org/10.1016/j.myc.2016.10.002>
- J.B. Chaires, N. Dattagupta and D.M. Crothers, *Biochemistry*, **21**, 3933 (1982); <https://doi.org/10.1021/bi00260a005>
- R. Bielski and G. Gryniewicz, *Green Chem.*, **23**, 7458 (2021); <https://doi.org/10.1039/D1GC02402G>
- T. Koopmans, *Physica*, **1**, 104 (1934); [https://doi.org/10.1016/S0031-8914\(34\)90011-2](https://doi.org/10.1016/S0031-8914(34)90011-2)
- R.G. Parr and R.G. Pearson, *J. Am. Chem. Soc.*, **105**, 7512 (1983); <https://doi.org/10.1021/ja00364a005>
- A. Mehta, A. Jain and G. Saxena, *Pharm. Biochem. Res.*, **8**, 301 (2022); <https://doi.org/10.32598/PBR.8.4.1067.1>
- Y. Deswal, S. Asija, D. Kumar, D.K. Jindal, G. Chandan, V. Panwar, S. Saroya and N. Kumar, *Res. Chem. Intermed.*, **48**, 703 (2022); <https://doi.org/10.1007/s11164-021-04621-5>
- O.M. Adly and H.F. El-Shafiy, *J. Coord. Chem.*, **72**, 218 (2019); <https://doi.org/10.1080/00958972.2018.1564912>
- L. McAfee, *J. Chem. Educ.*, **77**, 1122 (2000); <https://doi.org/10.1021/ed077p1122.1>
- R.A. Ammar, A.M. Alaghaz, M.E. Zayed and L.A. Albedair, *J. Mol. Struct.*, **1141**, 368 (2017); <https://doi.org/10.1016/j.molstruc.2017.03.080>
- N. Raman, K. Pothiraj and T. Baskaran, *J. Mol. Struct.*, **1000**, 135 (2011); <https://doi.org/10.1016/j.molstruc.2011.06.006>
- S.B. Jagtap, N.N. Patil, B.P. Kapadnis and B.A. Kulkarni, *Met. Based Drugs*, **8**, 159 (2001); <https://doi.org/10.1155/MBD.2001.159>
- M. Selvaganapathy, N. Pravin, K. Pothiraj and N. Raman, *J. Photochem. Photobiol. B*, **138**, 256 (2014); <https://doi.org/10.1016/j.jphotobiol.2014.06.003>
- W.J. Geary, *Coord. Chem. Rev.*, **7**, 81 (1971); [https://doi.org/10.1016/S0010-8545\(00\)80009-0](https://doi.org/10.1016/S0010-8545(00)80009-0)
- J.R.A. McLachlan, D.J. Smith, N.P. Chmel and A. Rodger, *Soft Matter*, **9**, 4977 (2013); <https://doi.org/10.1039/c3sm27419e>
- M. Sönmez, M. Celebi and I. Berber, *Eur. J. Med. Chem.*, **45**, 1935 (2010); <https://doi.org/10.1016/j.ejmech.2010.01.035>
- Q. Liang, P.D. Eason and E.C. Long, *J. Am. Chem. Soc.*, **117**, 9625 (1995); <https://doi.org/10.1021/ja00143a002>
- K. Uchida, A.M. Pyle, T. Morii and J.K. Barton, *Nucleic Acids Res.*, **17**, 10259 (1989); <https://doi.org/10.1093/nar/17.24.10259>
- A.W. Wallace, W. Rorer Murphy Jr. and J.D. Petersen, *Inorg. Chim. Acta*, **166**, 47 (1989); [https://doi.org/10.1016/S0020-1693\(00\)80785-9](https://doi.org/10.1016/S0020-1693(00)80785-9)
- G.M. Cohen and H. Eisenberg, *Biopolymers*, **8**, 45 (1969); <https://doi.org/10.1002/bip.1969.360080105>
- Ü. Demirbas, B. Barut, A. Özel, F. Çelik, H. Kantekin and K. Sancak, *J. Mol. Struct.*, **1177**, 571 (2019); <https://doi.org/10.1016/j.molstruc.2018.10.006>

37. N. Shahabadi, S. Kashanian and F. Darabi, *Eur. J. Med. Chem.*, **45**, 4239 (2010);
<https://doi.org/10.1016/j.ejmech.2010.06.020>
38. R. Ramesh and S. Maheswaran, *J. Inorg. Biochem.*, **96**, 457 (2003);
[https://doi.org/10.1016/S0162-0134\(03\)00237-X](https://doi.org/10.1016/S0162-0134(03)00237-X)
39. O.H. Al-Obaidi, *Open J. Inorg. Non-metallic Mater.*, **2**, 59 (2012);
<https://doi.org/10.4236/ojinm.2012.24007>
40. S.N. Shukla, P. Gaur, S.S. Bagri, R. Mehrotra and B. Chaurasia, *J. Serb. Chem. Soc.*, **86**, 269 (2021);
<https://doi.org/10.2298/JSC200902075S>
41. R. Firinci, *J. Mol. Struct.*, **1195**, 246 (2019);
<https://doi.org/10.1016/j.molstruc.2019.05.129>
42. Y.H. Hobani, A. Jerah and A. Bidwai, *Bioinformation*, **13**, 63 (2017);
<https://doi.org/10.6026/97320630013063>
43. E. Halevas, A. Pekou, R. Papi, B. Mavroidi, A.G. Hatzidimitriou, G. Zahariou, G. Litsardakis, M. Sagnou, M. Pelecanou and A.A. Pantazaki, *J. Inorg. Biochem.*, **208**, 111083 (2020);
<https://doi.org/10.1016/j.jinorgbio.2020.111083>
44. C.A. Lipinski, F. Lombardo, B.W. Dominy and P.J. Feeney, *Adv. Drug Deliv. Rev.*, **46**, 3 (2001);
[https://doi.org/10.1016/S0169-409X\(00\)00129-0](https://doi.org/10.1016/S0169-409X(00)00129-0)
45. D.F. Veber, S.R. Johnson, H. Cheng, B.R. Smith, K.W. Ward and K.D. Kopple, *J. Med. Chem.*, **45**, 2615 (2002);
<https://doi.org/10.1021/jm020017n>